Precise Wide Baseline Stereo Image Matching for Compact Digital Cameras

Martinus Edwin Tjahjadi
Department of Geodesy
National Institute of Technology (ITN) Malang
Malang, Indonesia
edwin@lecturer.itn.ac.id

Fourry Handoko
Department of Industrial Engineering
National Institute of Technology (ITN) Malang
Malang, Indonesia

***Abstract*— Numerous image matching methods for wide range of applications have been invented in the last decade. When high precision and reliability of the object space point coordinates is highly demanding, a stereo image matching method which can produce conjugate point of images and a standard deviation of the matched point is examined. In this approach, image gradients are used locally to seek a conjugate patch. The normalized cross correlation is first utilized to estimate an approximate location of the conjugate patch between two normalized images. Then the location of conjugate patch is further refined by using Gaussian-Newton least squares image matching. Both radiometric and geometric parameters of least squares models are used selectively in seeking the best possible accuracy. Iterative computation is conducted to incrementally refine the geometric location of the conjugate point. After a matched patch has been found, a variant-covariant matrix of the parameter is analyzed to inform the precision of the conjugate points both on images and object space. This method can compute high precision object space points and some examples demonstrate the insight of the approach.**

Keywords*— *Image Matching; Rectification; Least Squares Adjustment; Stereo pair; image processing

I. INTRODUCTION

A method of extracting discrete object surface points from a low altitude aerial photography or from photographed industrial objects features is extensively researched [1]. Area-based least square image matching methods are successfully implemented in digital photogrammetry and computer vision [2] Albeit widely applied image matching, least squares image matching (LSM) still has a persistent unsolved rudimentary problem in general terms [3]. Five aspects affect the solution of LSM [4], namely the window template, texture, functional model, geometric distortion and initial values.

The terms "image matching" refers to the proses of finding corresponding or conjugate points in digital images or part thereof in the form of a matrix of reflectance levels [5]. The concept of LSM is to minimize the grey level differences between the reference patch and the target patch (Fig. 1) whilst computing the position and the shaping parameters of the target patch during the least squares estimation process. Therefore, the position and the shape of the target patch are both varied until the grey level differences between the deformed target patch and the template patch reach a minimum.

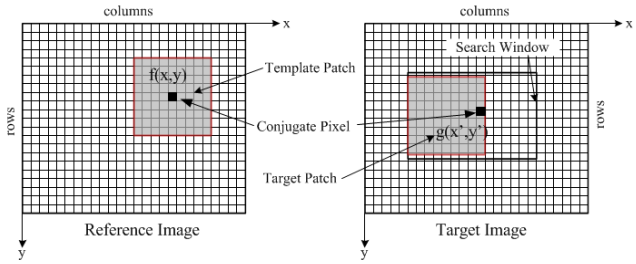

Fig. 1. The concept of least square image matching

Wide baseline stereo image matching usually encounter with geometric and radiometric differences between images such as scale and perspective difference, different lighting condition [6, 7] and high frequency contaminations [8]. While this situation occurs, an image matching using a prominent method like a normalized cross correlation [9] often produces a misleading match and it is error prone. These disadvantages underpin a concept of solution which needs to account for geometric and radiometric differences between patches in order to seek a better match.

Therefore, this paper discusses an alternative method to alleviate geometric distortions and initial value problems for a wide baseline stereo pair. By assuming exterior and interior orientation parameters of the stereo images are known, normalized stereo images[10] are created as the intermediate process to reduce the geometric differences and to facilitate a close approximation to start the LSM on the wide baseline image pair. This concept is set up in the context of least square estimations. A normalized cross correlation method is first utilized on the normalized pair to find a true match. Then positions of the matched conjugate points are transformed as an approximate value of the LSM on the original images (i.e. wide baseline stereo images) to minimize a pull in range problem and to obtain a precise final matched point.

II. RESEARCH METHOD

The LSM employs iterative radiometric and geometric transformation between patches. If f(x, y) in Fig. 1 is to be a template patch of n x n pixels and g(x, y) is to be a target patch of an equal size, the objective of the LSM is to estimate a new

Ministry of Research, Technology and Higher Education of the Republic Indonesia.

location of g(x, y) such that grey value differences between them are minimized. In an ideal situation where noise free patches exist, matching is established if the following condition is met [4, 11]:

$$f(x,y) = g(x',y'); \qquad \begin{aligned} x' &= a_0 + a_1 x + a_2 y \\ y' &= b_0 + b_1 x + b_2 y \end{aligned} \tag{1}$$

In which the two patches coordinate system are related by affine transformation which is considered to be a sufficient parameter set as the size of the patches correspond to a relatively small plane area of the object in object space [11]. To compensate temporal differences of illumination source radiance, different distance and viewing angles of the cameras to the object, and errors in imaging acquisition, two radiometric parameters for brightness r_o (i.e. grey value shift) and contrast r_1 (i.e. grey value scale) are introduced to the target patch in the form of a condition equation:

$$f(x,y) = r_o + r_1\, g(x',y'); \; F \equiv f(x,y) - r_o - r_1\, g(x',y') = 0 \tag{2}$$

Where f(x, y) are considered as vector of observations, g(x', y') are constant terms, and the parameters are a_1, a_2, a_3, b_1, b_2, b_3, r_o, and r_1. This equation can be linearized with respect to the parameters into the form of standard indirect model for n x n pixels of a template patch:

$$_{nxn}\mathbf{v}_1 + {}_{nxn}\mathbf{B}_{8\,8}\boldsymbol{\Delta}_1 = {}_{nxn}\mathbf{f}_1 \tag{3}$$

Here $\boldsymbol{\Delta}$ is the vector of corrections to approximate parameter values, **f** is the discrepancy vector constant between the patches, **v** is the vector of noise values between patches and it can also be regarded as a measure of the quality of the mathematical model, **B** is the matrix of coefficients and it contains the partial derivatives of (2):

$$\mathbf{B} = \left[\frac{\partial F}{\partial a_0} \;\; \frac{\partial F}{\partial a_1} \;\; \frac{\partial F}{\partial a_2} \;\; \frac{\partial F}{\partial b_0} \;\; \frac{\partial F}{\partial b_1} \;\; \frac{\partial F}{\partial b_2} \;\; \frac{\partial F}{\partial r_0} \;\; \frac{\partial F}{\partial r_1} \right] \tag{4}$$

The partial derivatives of (2) and the right hand side term for 1 pixel can be elaborated in (5a) – (5f), (6) and (7) as follows:

$$\partial F/\partial a_0 = -r_1\; dg(x',y')/dx'\; dx'/da_0 = -g_x \tag{5a}$$

$$\partial F/\partial a_1 = -r_1\; dg(x',y')/dx'\; dx'/da_1 = -g_x x \tag{5b}$$

$$\partial F/\partial a_2 = -r_1\; dg(x',y')/dx'\;\; dx'/da_2 = -g_x y \tag{5c}$$

$$\partial F/\partial b_0 = -r_1\; dg(x',y')/dy'\; dy'/db_0 = -g_y \tag{5d}$$

$$\partial F/\partial b_1 = -r_1\; dg(x',y')/dy'\; dy'/db_1 = -g_y x \tag{5c}$$

$$\partial F/\partial b_2 = -r_1\; dg(x',y')/dy'\; dy'/db_2 = -g_y y \tag{5d}$$

$$\partial F/\partial r_0 = -1; \;\; \partial F/\partial r_1 = -g(x',y') \tag{5e}$$

$$\mathbf{f} = -F = -(f(x,y) - r_o - r_1\, g(x',y')) \tag{5f}$$

$$_8\boldsymbol{\Delta}_1 = [\delta a_0 \;\; \delta a_1 \;\; \delta a_2 \;\; \delta b_0 \;\; \delta b_1 \;\; \delta b_2 \;\; r_0 \;\; r_1]^T \tag{6}$$

$$\mathbf{v} = -g_x \delta a_0 - g_x x \delta a_1 - g_x y \delta a_2 - g_y \delta b_0 - g_y x \delta b_1 - g_y y \delta b_2 - F \tag{7}$$

where

$$g_x = dg(x',y')/dx' = g(x'+1,y') - g(x'-1,y')/2 \tag{8a}$$

$$g_y = dg(x',y')/dy' = g(x',y'+1) - g(x',y'-1)/2 \tag{8b}$$

The g_x in (8a) and g_y in (8b) are a discrete first derivative (i.e. a gradient) in the x-direction and in the y-direction, respectively. Values of g_x and g_y are evaluated as the slopes of the reflectance levels in the x and y directions across the initial target patch before performing iteration, and across the transformed target patch thereafter. A conversion from color images to gray value images are based upon Zhou and Boulanger's recommendations [12]. The least squares solution minimizes the sum squares of the element of **v**, which leads to the unbiased minimum variance estimators and gives:

$$\boldsymbol{\Delta} = (\mathbf{B}^T\mathbf{P}\mathbf{B})^{-1}\mathbf{B}^T\mathbf{P}\mathbf{f}; \quad \hat{\mathbf{x}} = \mathbf{x}^o + \boldsymbol{\Delta} \tag{9a}$$

$$\hat{\sigma}_0^2 = \mathbf{v}^T\mathbf{P}\mathbf{v}/n\,x\,n - 8; \; \mathbf{C}_x = \hat{\sigma}_0^2(\mathbf{B}^T\mathbf{P}\mathbf{B})^{-1} \tag{9b}$$

In (9a) and (9b) **P** is the weight matrix which is usually approximated by the identity matrix by assuming an identical precision of all pixels; n is the number of pixel in row or column direction; $\hat{\mathbf{x}}$ is the solution vector; $\boldsymbol{\Delta}$ is the correction vector which is applied for the geometric transformation parameters only; r_o and r_1 are linear apriori; and $\hat{\sigma}_o$ can be regarded as a posteriori estimator for the difference of the template patch noise and the target patch noise. $\mathbf{C}_\mathbf{x}$ is the variance-covariance matrix of the transformation parameters and it is used to judge the quality of parameter estimation.

Since the function values of g(x', y') in (1) are stochastic quantities, the design matrix of **B** is not fixed, but ignoring it does not significantly disturb the results [13]. Therefore, a complete set of matrix elements for n x n pixels of template patch can be rewritten as follows:

$$
{}_{nxn}\mathbf{B}_8 = \begin{bmatrix}
-g_{x_1} & -g_{x1}x_1 & -g_{x_1}y_1 & -g_{y_1} \\
-g_{x_2} & -g_{x2}x_2 & -g_{x_2}y_1 & -g_{y_1} \\
\vdots & \vdots & \vdots & \vdots \\
-g_{x_n} & -g_{xn}x_n & -g_{x_n}y_1 & -g_{y_2} \\
-g_{x_1} & -g_{x1}x_1 & -g_{x_1}y_2 & -g_{y_2} \\
\vdots & \vdots & \vdots & \vdots \\
-g_{x_n} & -g_{x_n}x_n & -g_{x_n}y_2 & -g_{y_2} \\
\vdots & \vdots & \vdots & \vdots \\
-g_{x_{n-1}} & -g_{x_{n-1}}x_{n-1} & -g_{x_{n-1}}y_n & -g_{y_n} \\
-g_{x_n} & -g_{x_n}x_n & -g_{x_n}y_n & -g_{y_n}
\end{bmatrix}
\begin{bmatrix}
-g_{y_1}x_1 & -g_{y_1}y_1 & -1 & -g'(x_1,y_1) \\
-g_{y_1}x_2 & -g_{y_1}y_1 & -1 & -g'(x_2,y_1) \\
\vdots & \vdots & \vdots & \vdots \\
-g_{y_1}x_n & -g_{y_1}y_1 & -1 & -g'(x_n,y_1) \\
-g_{y_2}x_1 & -g_{y_2}y_2 & -1 & -g'(x_1,y_2) \\
\vdots & \vdots & \vdots & \vdots \\
-g_{y_2}x_n & -g_{y_2}y_2 & -1 & -g'(x_n,y_2) \\
\vdots & \vdots & \vdots & \vdots \\
-g_{y_n}x_{n-1} & -g_{y_n}y_n & -1 & -g'(x_{n-1},y_{n-1}) \\
-g_{y_n}x_n & -g_{y_n}y_n & -1 & -g'(x_{n-1},y_{n-1})
\end{bmatrix} \quad (10)
$$

$$
{}_{nxn}\mathbf{f}_1 = \begin{bmatrix}
-\left(f(x_1,y_1) - r_o - r_1\, g(x'_1,y'_1)\right) \\
-\left(f(x_2,y_1) - r_o - r_1\, g(x'_2,y'_1)\right) \\
\vdots \\
-\left(f(x_n,y_1) - r_o - r_1\, g(x'_n,y'_1)\right) \\
-\left(f(x_1,y_2) - r_o - r_1\, g(x'_1,y'_2)\right) \\
\vdots \\
-\left(f(x_n,y_2) - r_o - r_1\, g(x'_n,y'_2)\right) \\
\vdots \\
-\left(f(x_{n=1},y_n) - r_o - r_1\, g(x'_{n-1},y'_n)\right) \\
-\left(f(x_n,y_n) - r_o - r_1\, g(x'_n,y'_n)\right)
\end{bmatrix} \quad (11)
$$

$$
{}_{nxn}\mathbf{v}_1 = \begin{bmatrix}
-g_{x_1}\delta a_0 - g_{x_1}x_1\delta a_1 - g_{x_1}y_1\delta a_2 \\
-g_{x_2}\delta a_0 - g_{x_2}x_2\delta a_1 - g_{x_2}y_1\delta a_2 \\
\vdots \\
-g_{x_n}\delta a_0 - g_{x_n}x_n\delta a_1 - g_{x_n}y_1\delta a_2 \\
-g_{x_1}\delta a_0 - g_{x_1}x_1\delta a_1 - g_{x_1}y_2\delta a_2 \\
\vdots \\
-g_{x_n}\delta a_0 - g_{x_n}x_n\delta a_1 - g_{x_n}y_2\delta a_2 \\
\vdots \\
-g_{x_{n-1}}\delta a_0 - g_{x_{n-1}}x_{n-1}\delta a_1 - g_{x_{n-1}}y_n\delta a_2 \\
-g_{x_n}\delta a_0 - g_{x_n}x_n\delta a_1 - g_{x_n}y_n\delta a_2
\end{bmatrix}
\begin{bmatrix}
-g_{y_1}\delta b_0 - g_{y_1}x_1\delta b_1 - g_{y_1}y_1\delta b_2 - F_{1,1} \\
-g_{y_1}\delta b_0 - g_{y_1}x_2\delta b_1 - g_{y_1}y_1\delta b_2 - F_{2,1} \\
\vdots \\
-g_{y_1}\delta b_0 - g_{y_1}x_n\delta b_1 - g_{y_1}y_1\delta b_2 - F_{n,1} \\
-g_{y_2}\delta b_0 - g_{y_2}x_1\delta b_1 - g_{y_2}y_2\delta b_2 - F_{1,2} \\
\vdots \\
-g_{y_2}\delta b_0 - g_{y_2}x_n\delta b_1 - g_{y_2}y_2\delta b_2 - F_{,n2} \\
\vdots \\
-g_{y_n}\delta b_0 - g_{y_n}x_{n-1}\delta b_1 - g_{y_n}y_n\delta b_2 - F_{n-1,n} \\
-g_{y_n}\delta b_0 - g_{y_n}x_n\delta b_1 - g_{y_n}y_n\delta b_2 - F_{n,n}
\end{bmatrix} \quad (12)
$$

It is noteworthy precaution that the adjustment procedure for the LSM is somewhat different from the usual iteration cycle of a least squares adjustment. Since it is assumed that the stereo images are nearly aligned and are radiometrically similar, the first iteration commences with an approximate location of the target patch. The coefficient of the design matrix **B** in (10) and discrepancy vector **f** in (11) are calculated using initial values of parameters to initiate the iteration. These initial values are often $a_0=b_0=a_2=b_1=r_o=0$; and $a_1=b_2=r_1=1$.

III. Result And Analysis

The experimental testing starts by selecting two overlapping images which have substantial differences of viewing angles (Fig. 2) to meet the criteria of wide baseline stereo images. The presumably known exterior and interior orientation parameters are utilized to generate the normalized pair of stereo images (Fig. 3) [10, 14]. This normalized pair is used to approximate position of a clicked pixel on the target image that need to be located as close as possible to its true value, possibly around 1-2 pixels. An automatic method of finding this approximate pixel location on the target image is developed in this research through a utilization of the normalized stereo pair.

A normalized stereo pair is characterized by both of the normalized images have a zero parallax in y-axis direction [9, 15]. Hence, conjugate pixel locations on the normalized images have an equal row value (i.e. an equal y coordinate value). This condition is met when the two camera axes of a stereo image pair parallel to each other and perpendicular to the camera base [10, 16]. Therefore, the conjugate points have zero y-parallax,

and a searching of matching entities is confined to pixels along the x direction only.

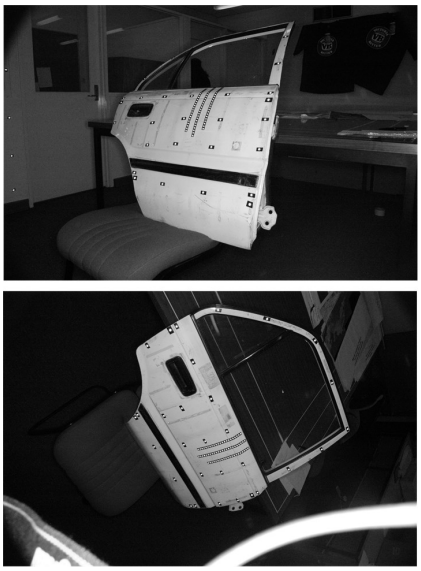

Fig. 2. Input of Stereo images: A reference image (top) and a target image (bottom).

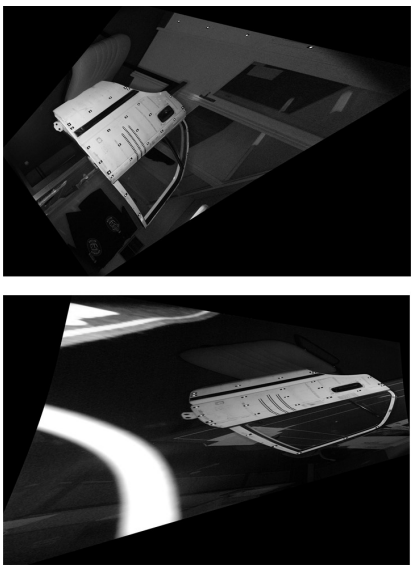

Fig. 3. A normalized reference image (top) and a normalized target image (bottom)

In a developed program, the process of an interactive image matching starts by selecting a pixel on the reference image, e.g. retro targets features (Fig. 4). A selected template patch centered at the clicked pixel is automatically processed. Sizes of the chosen patch are determined based on [17, 18]. A position of the clicked pixel is transformed to the normalized reference image (Fig. 5) to seek the corresponding pixel as pointed out by [10].

Now, an automatic finding of the conjugate point on the normalized target image is triggered (Fig. 6). Here the y coordinate of the pixel on the normalized reference image is used to determine the row on the normalized target image. The transformed x coordinates of the two ends of the epipolar line are used to determine the minimum and maximum column of the epipolar line (i.e. a horizontal line) on the normalized target image. Then, the normalized cross correlation method is performed at every pixel on the row at a specified numbers of column (pixels) on the normalized target image. The number of pixels computed on the row is determined by the length of the epipolar line, which is based on the minimum and maximum values of the coordinates of the available data points. Since the rows are epipolar lines in the normalized images (Fig. 5 and 6), the automatic matching procedure for conjugate points can be performed on the same row (y-coordinate).

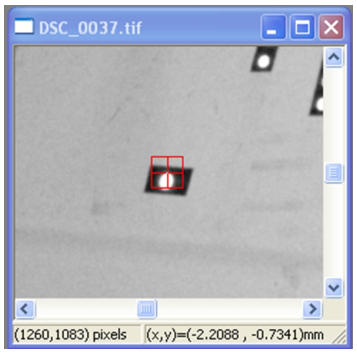

Fig. 4. Template patch on the reference image.

Fig. 5. Template patch on the normalized reference image.

To seek a sub-pixel accuracy of the matched point, the LSM is conducted (Fig. 7 and Table I). Since the LSM requires very close approximate values (small pull in range), the pixel coordinates calculated from the cross correlation method on the normalized target patch are transformed back to the target image to obtain the approximate pixel coordinates. Then, the coordinates are rounded up to the nearest integer values. A patch, whose size is equal to the one selected on the reference digital image centered at this pixel coordinates, is retrieved. A pair of patches (Fig. 4 and Fig. 7) and their center pixel coordinates are incorporated to perform the LSM.

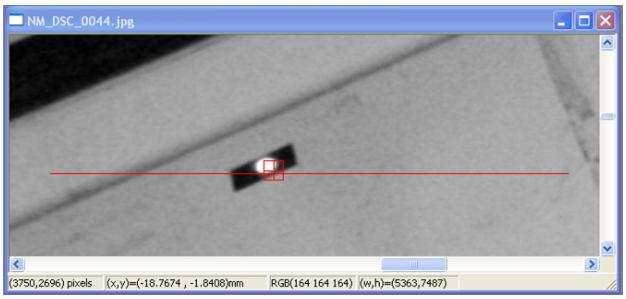

Fig. 6. Target patch on the normalized target image. An approximate conjugate point is resulted from normalized cross correlation matching method. A red line is an epipolar line.

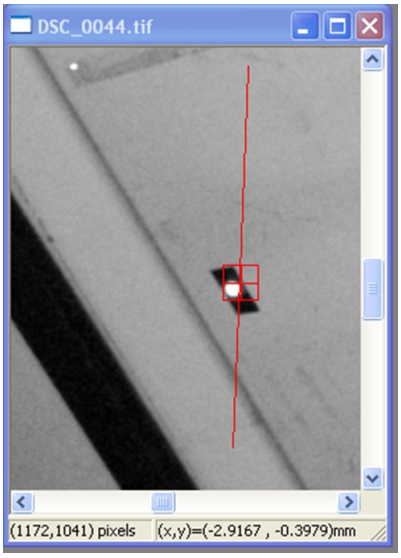

Fig. 7. Target patch on the target image. A precise conjugate point is resulted from the LSM method. A search for correspondence is confined along the epipolar line (red line).

The template patch is obtained by clicking its center pixel on the reference image (Fig. 4). A center pixel of the initial target patch in Fig. 7 is an approximate pixel obtained from the cross correlation on the normalized image pair (Table I.1). During the LSM's iterations (Table I (1) – (8)), the target patch is transformed incrementally into the template patch. On the last iteration (Table I (8)), therefore, the target patch resembles the template patch; and its center pixel is to be the conjugate point on the target patch. The iterative LSM processes are summarized in Table I.

The adjustment equation of (9a) for the LSM is usually very over determined. For example, a patch size of 21x21 pixels generates n = 441 observations for only 8 unknowns. Grey level gradients are used in the linearized correction equations, i.e. (3). A solution exists only if enough image structures (edges) are available in the matched patch shown in Table II (f); while for homogeneous textures of image patches, the normal equation system is singular, which is the situation illustrated in Table II (e). If the conjugate pixels coordinates are obtained, the corresponding conjugate point can also be triangulated in the object space.

TABLE I. ITERATIVE TRANSFORMATION OF THE INITIAL TARGET PATCH ON THE TARGET IMAGE. IT IS GEOMETRICALLY AND RADIOMETRICALLY TRANSFORMED AND WARPED TO RESEMBLE A TEMPLATE PATCH ON THE REFERENCE IMAGE

LSM's Iteration Index	Warped Patch	
	Iterated Target Patch	Start/End Patch
1	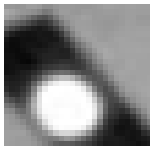 (Initial Target Patch on Fig.7)	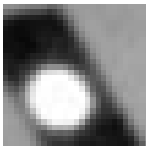 (Initial Target Patch on Fig.7)
2	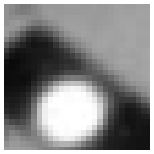	Incremental warping of initial target patch into template patch
3	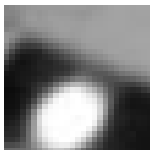	
4		
5		
6	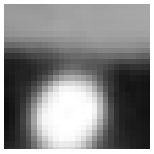	
7	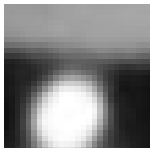	
8	 (Warped Target Patch)	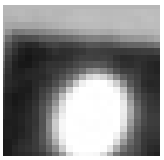 (Template Patch on Fig. 4)

A typical result of standard deviations of the matched pixels and its triangulated points is shown in Table II. Here, the shift parameters of a_0 and b_0 only are shown for the LSM method. The standard deviations of shift parameters a_0 and b_0 are assessed to judge the accuracy of the matched points and the highest possible accuracies have been reported to be in the

range of 0.01-0.04 pixels. High accuracy assumes good similarity between the template and the target patch. A typical result of standard deviations of the a_0 and b_0 calculated by the software developed for this research is depicted in Table II (a-d). Once matched, the conjugate points can be triangulated to generate object space coordinate of those ones with high precision. For poor texture patches, the LSM process might failed, hence the object space coordinate cannot be produced, shown in Table II (e-f).

TABLE II. THE LSM ON VARIOUS PATCHES AND THE ACCURACIES OF THE MATCHED AND TRIANGULATED POINTS.

No	Patch	Precision Patch (in pixels)		Precision of triangulated Point (in mm)		
(1)	(2)	(3)		(4)		
		σ_{ao}	σ_{bo}	σ_X	σ_Y	σ_Z
a		0.05296	0.07029	0.07775	0.06619	0.08766
b		0.03367	0.14962	0.45721	0.38797	0.55291
c		0.06922	0.12099	0.64647	0.50791	0.73545
d		0.06296	0.13464	0.26252	0.21888	0.31255
e		Not Available (Poor Texture)		None		
f		Not Convergent		None		

IV. CONCLUSION

This paper has presented an interactive and semi-automatic method used to produce XYZ object point coordinates from the LSM process for the wide baseline stereo pair. The process starts by selecting a pixel on the template image. Then, the program can be used to automatically find its conjugate point on the target image, as well as the corresponding point in the object space. The automatic searching of the matched point is done in two processes. The first process is performed on the normalized image pair to compute the matched point using cross correlation matching. Using the matched point on the normalized matching image as an approximate value, the second process is performed on the original image pair to refine the matched point position on the target image to obtain sub-pixel accuracy of the matched point through the LSM method. This method can reliably compute high precision object space points from a wide baseline stereo pair.

ACKNOWLEDGMENT

The author wishes to express his sincere thanks to Ministry of Research, Technology and Higher Education of the Republic of Indonesia for supporting a research grant "*Penelitian Terapan Unggulan Perguruan Tinggi (PTUPT)*", with an announcement letter number 025/E3/2017 and a contract number 073/SP2H/K2/KM/2017.

REFERENCES

[1] M. E. Tjahjadi, F. Handoko, and S. S. Sai, "Novel Image Mosaicking of UAV's Imagery Using Collinearity Condition," International Journal of Electrical and Computer Engineering (IJECE), vol. 7(3) , pp. 1188-1196, June 2017.

[2] A. Gruen, "Development and status of image matching in photogrammetry," The Photogrammetric Record, vol. 27(137), pp. 36-57, 2012.

[3] H. Yu, Y. Fang, L. Kong, and X. Wang, "Stereo Matching Based on Least Square," International Journal of Multimedia & Ubiquitous Engineering, vol. 10(2), pp. 395-403, 2015.

[4] Z. Li and J. Wang, "Least squares image matching: A comparison of the performance of robust estimators," ISPRS Annals of Photogrammetry, Remote Sensing and Spatial Information Sciences, vol. 2(1), pp. 37-44, 2014.

[5] L. Pilgrim, "Two Dimensional Image Matching and Difference Detection," Australian Journal of Geodesy, Photogrammetry and Surveying, vol. (56), pp. 1-36, June 1992.

[6] H. L. Mitchell, "An Outline of Least Squares Image Matching in Digital Photogrammetry," in First Australian Photogrammetric Conference, Sydney, Australia, 1991, Unpaginated paper: 10 p.

[7] J. C. Trinder, T. Tjugiarto, and B. E. Donnelly, "A Digital Photogrammetry System for Close Range," Australian Journal of Geodesy, Photogrammetry and Surveying, vol. (53), pp. 1-13, December 1990.

[8] H. Bischof and F. Leberl, "Digital Image Processing," in Manual of Photogrammetry: 6th Edition, J. C. McGlone, Ed., Bethesda, Maryland: American Society for Photogrammetry and Remote Sensing, 2013, pp. 451-515.

[9] H. Mayer, M. Sester, and G. Vosselman, "Basic Computer Vision Technique," in Manual of Photogrammetry 6th Edition, J. C. McGlone, Ed., Bethesda, Maryland: American Society for Photogrammetry and Remote Sensing, 2013, pp. 517-583.

[10] M. E. Tjahjadi, F. Handoko, and S. S. Sai, "Precise Stereo Image Rectification for Consumer Grade Digital Cameras," International Journal of Electrical and Computer Engineering (IJECE), in Press.

[11] A. W. Gruen, "Adaptive Least Squares Correlation: A Powerful Image Matching Technique," South African Journal of Photogrammetry, Remote Sensing and Cartography, vol. 14(3), pp. 175-187, 1985.

[12] X. Zhou and P. Boulanger, "Radiometric invariant stereo matching based on relative gradients," in 19th IEEE International Conference on Image Processing (ICIP), 2012, pp. 2989-2992.

[13] A. W. Gruen, "Least Square Matching: A Fundamental Measurment Algorithm," in Close Range Photogrammetry and Machine Vision, K. B. Atkinson, Ed., Scotland, UK: Whittles Publishing, 2001, pp. 217-255.

[14] M. E. Tjahjadi, "A Fast And Stable Orientation Solution of Three Cameras-Based UAV Imageries," ARPN Journal of Engineering and Applied Sciences, vol. 11(5), pp. 3449-3455, March 2016.

[15] S. Liansheng, Z. Jiulong, and C. Duwu, "Image rectification using affine epipolar geometric constraint," Journal of Software, vol. 4(1), p. 26-33, February 2009.

[16] W. Cho and T. Schenk, "Resampling Digital Imagery to Epipolar Geometry," International Archives of Photogrammetry and Remote Sensing, vol. 29(B3), pp. 404-408, 1992.

[17] A. Alba, J. F. Vigueras-Gomez, E. R. Arce-Santana, and R. M. Aguilar-Ponce, "Phase correlation with sub-pixel accuracy: A comparative study in 1D and 2D," Computer Vision & Image Understanding, vol. 137, pp. 76-87, March 2015.

[18] Y. He, P. Wang, and J. Fu, "An Adaptive Window Stereo Matching Based on Gradient," 3rd International Conference on Electric and Electronics (EEIC), 2013, pp. 437-440.